

Identification of novel split-GAL4 drivers for the characterization of enteroendocrine cells in the *Drosophila melanogaster* midgut

Jessica M. Holsopple , Kevin R. Cook , *Ellen M. Popodi 

Department of Biology, Bloomington Drosophila Stock Center, Indiana University, Bloomington, IN 47405, USA

*Corresponding author: Department of Biology, Bloomington Drosophila Stock Center, Indiana University, Bloomington, IN 47405, USA. Email: kercook@indiana.edu

Abstract

The *Drosophila melanogaster* midgut is commonly studied as a model epithelial tissue for many reasons, one of which is the presence of a diverse population of secretory cells called enteroendocrine cells. Subpopulations of these cells secrete various combinations of peptide hormones which have systemic effects on the organism. Many of these hormones are also produced in the *Drosophila* brain. The split-GAL4 system has been useful for identifying and manipulating discrete groups of cells, but previously characterized split-GAL4 drivers have not driven expression in high proportions of enteroendocrine cells. In this study, we screened candidate split-GAL4 drivers for enteroendocrine cell expression using known reference drivers for this cell type and discovered a new split-GAL4 driver pair that confers expression in a greater number of enteroendocrine cells than previously characterized driver pairs. The new pair demonstrates less brain expression, thereby providing better tools for disentangling the physiological roles of gut- and brain-secreted peptides. We also identified additional split-GAL4 drivers that promote expression in discrete subpopulations of enteroendocrine cells. Overall, the tools reported here will help researchers better target enteroendocrine cell subpopulations.

Keywords: *Drosophila*; intestine; gut; midgut; split-GAL4; endocrine; enteroendocrine cell

Introduction

The *Drosophila melanogaster* intestine is a widely studied model tissue due to its many parallels to mammalian digestive systems, the extensive genetic manipulations available in *Drosophila*, and the simplicity of the tissue relative to the digestive tracts of other organisms (Zwick et al. 2019). The *Drosophila* intestine has 3 distinct regions: the foregut, midgut, and hindgut. Of these regions, the midgut is the most commonly studied. The midgut epithelium is made up of 4 cell types: intestinal stem cells (ISCs), their differentiating daughters called enteroblasts (EBs) (together termed progenitor cells), and 2 terminally differentiated cell types consisting of absorptive enterocytes (ECs) and secretory enteroendocrine cells (EEs) (Ohlstein and Spradling 2006; Miguel-Aliaga et al. 2018). Despite the relatively uncomplicated nature of this tissue, it provides functions similar to those of the mammalian stomach and small intestine.

As an important interface with the environment, the intestine must have the ability to adapt to rapidly changing conditions, such as feeding, starvation, and ingestion of toxins or pathogenic bacteria. To coordinate these adaptations, the *Drosophila* midgut uses diverse combinations of hormone secretions from EEs to communicate with cells both within the midgut and in other body regions (Veenstra et al. 2008; Veenstra and Ida 2014). RNAseq studies have shown that single EE cells can secrete combinations of up to 5 different peptide hormones, a fact that lends

itself to categorizing subpopulations of EEs based on the hormones secreted (Guo et al. 2019). Hormone secretion patterns are often regionalized, with subsets of EEs appearing in distinct portions of the intestine (Veenstra et al. 2008; Veenstra and Ida 2014; Guo et al. 2019; Hung et al. 2020). To date, there are few reagents available to manipulate discrete subpopulations of EEs.

The UAS-GAL4 system is a powerful tool of modern *Drosophila* research but GAL4 drivers unfortunately often lack the specificity needed to identify and manipulate small groups of cells, such as specific EE subtypes. To increase resolution, researchers have embraced the split-GAL4 system, in which expression of the GAL4 activation domain (AD) is controlled by different regulatory sequences than expression of the GAL4 DNA-binding domain (DBD). When both the AD and the DBD are expressed in the same cell, these domains can bind via attached leucine zipper tags to reconstitute functional GAL4, which can then activate expression of UAS transgenes (Luan et al. 2006). Because functional GAL4 is produced only when both domains are expressed together, this system allows for more fine-tuned patterns of UAS activation than the original UAS-GAL4 system. In this study, drivers contained the activation domain from the p65 gene (p65AD) in place of GAL4AD because p65AD induces stronger transcriptional activation (Dionne et al. 2018).

To improve the utility of the split-GAL4 system, recent work characterized the expression patterns of 7,304 experimental

Received: December 20, 2021. Accepted: April 18, 2022

© The Author(s) 2022. Published by Oxford University Press on behalf of Genetics Society of America.

This is an Open Access article distributed under the terms of the Creative Commons Attribution License (<https://creativecommons.org/licenses/by/4.0/>), which permits unrestricted reuse, distribution, and reproduction in any medium, provided the original work is properly cited.

split-GAL4 drivers in the *Drosophila* midgut by both cell type and region via 2 distinct screens (Ariyapala et al. 2020). First, experimental AD or DBD split-GAL4 drivers were combined with DBD or AD reference drivers known to direct expression only in the intestinal epithelium. Experimental drivers that did not direct expression in the midgut were not screened further. Drivers that did direct midgut expression were combined with appropriate AD or DBD reference drivers specific to each of the major midgut cell types (progenitor cells, ECs, or EEs) in a second screen to determine the unique cell-type expression profiles of each experimental split-GAL4 driver. The expression profiles of the intestine-specific reference drivers used in the first screen allowed for detection of high percentages of total midgut ISCs, EBs, and ECs, but a much lower percentage of EEs. Similarly, the reference drivers used in the second screen for recognition of progenitor cells and ECs enabled detection of a high percentage of their respective cell types, while the EE reference drivers facilitated detection of only half of EEs. These reference drivers were useful in characterizing the expression patterns of experimental drivers, but their weaknesses with respect to EEs suggest that many split-GAL4 drivers directing expression in EEs were overlooked by these screens. Reference drivers expressing in a higher proportion of EEs are needed to advance the study of this important cell type.

In *Drosophila*, a subset of neuropeptides produced in the brain are also produced by midgut EE cells (Nüssel and Winther 2010). For studies of neuropeptide signaling, it would be advantageous for split-GAL4 reference drivers expressed in EEs to be characterized in the brain. Ideally, drivers could be identified that allow the experimental manipulation of neuropeptide secretion specifically in EEs.

Here, we report the identification of a more sensitive and specific pair of EE reference drivers. The AD and DBD drivers share the same enhancer fragment, and we used them to identify and characterize 43 additional EE drivers that had been missed in previous screens. Our preliminary analysis suggests that the new driver pair activates less UAS reporter expression in the brain than the previously used EE reference drivers, which should prove beneficial to future studies of neuropeptide-related physiology.

Materials and methods

Drosophila strains and husbandry

Fly strains were cultured at 25° on standard Bloomington media (<https://bdsc.indiana.edu/information/recipes/bloomfood.html>). The genotypes of all starting stocks used in this study are listed in [Supplementary Table 1](#). The PBac{UAS-DSCP-6XEGFP}VK00018 strain used for reporter comparisons was a gift from Steve Stowers (Montana State University).

Dissections and immunostaining

To analyze the fluorescence from UAS-*Stinger* and *lexAop-tdTomato*, adult gastrointestinal tracts were dissected, fixed, and counterstained with DAPI as described in Ariyapala et al. (2020). Intestines from selected adults were antibody stained as described in Ariyapala et al. (2020) using primary mouse anti-Prospero (Pros) (MR1A, 1:100; Developmental Studies Hybridoma Bank) or rabbit anti-GFP (A-11122, Life Technologies, 1:1,000) antibody, and secondary AlexaFluor 568-conjugated goat anti-mouse or AlexaFluor 488-conjugated goat anti-rabbit antibody (A-11034 1:1,000; Life Technologies). In some cases, rhodamine-conjugated goat anti-Horseradish Peroxidase (HRP) antibody (123-025-021, 1:500; Jackson ImmunoResearch) was included

during secondary antibody staining. When only anti-HRP was used, intestines were dissected and fixed as described in Ariyapala et al. (2020), washed 3 times in PBT [0.1% Triton X-100 in PBS (137 mM NaCl, 2.68 mM KCl, 10.1 mM Na₂HPO₄, and 1.76 mM KH₂PO₄, pH 7.4)], blocked in 0.5% bovine serum albumin and 5% normal goat serum in PBT for 1 h, incubated with DAPI and anti-HRP overnight, washed 5 times in PBT and mounted with VectaShield Plus mounting medium (Vector Laboratories, Burlingame, CA, USA).

Adult brains were prepared following the same protocol of fixation, washing, and DAPI staining used for gut dissection. No antibody staining was performed on adult brains.

Microscopy and image processing

Images of whole dissected intestines and brains were taken on a Zeiss Axio Zoom microscope. Images of immunostained intestines for quantification were taken on a Zeiss Axio Observer microscope. Image files were prepared using Adobe Photoshop and figures were assembled using Adobe Illustrator.

Expression pattern and statistical analyses

When screening for EE expression, the numbers of cells expressing UAS-*Stinger* in each of the 11 intestinal subregions (Buchon et al. 2013) were scored semiquantitatively from the intestines of five 4- to 8-day-old adult female flies using the method described in Ariyapala et al. (2020). When precise cell numbers were determined, 8 intestines were analyzed. When screening for brain expression, brains of five 4- to 8-day-old adult females were dissected and scored.

Statistical analyses were performed in Excel and graphs were made using GraphPad Prism Version 6. For each comparison, midgut regions were evaluated independently using a chi-squared test. Brain data were also analyzed using a chi-squared test.

Results and discussion

Screening for split-GAL4 drivers with extensive, enteroendocrine cell-specific expression

To expand the number of split-GAL4 driver combinations useful for EE cell studies, we screened a selection of split-GAL4 drivers using the EE reference drivers P{R57F07-p65.AD.A} and P{R57F07-GAL4.DBD.A} generated by Ariyapala et al. (2020). We will differentiate these drivers from the similar P{R57F07-p65.AD} and P{R57F07-GAL4.DBD} drivers generated at Janelia Research Campus (Dionne et al. 2018) by referring to them as R57F07.A-p65AD and -GAL4DBD. [Supplementary Fig. 1](#) shows the difference in midgut expression patterns between the R57F07 and R57F07.A split-GAL4 driver pairs, as well as additional characterization of the R57F07.A driver pair. To find new EE reference drivers that capture broader EE expression than the R57F07.A drivers, we screened drivers from 3 nonexclusive categories ([Supplementary Table 2](#)): (1) 42 drivers with enhancer fragments previously reported to direct expression in EEs in either GAL4 or split-GAL4 constructs (Marianes and Spradling 2013; Beehler-Evans and Micchelli 2015; Guo et al. 2019; Lim et al. 2021); (2) 13 drivers with enhancer fragments found by Ariyapala et al. (2020) to direct reporter expression only in EEs (some drivers were characterized previously, while others drivers shared an enhancer fragment with a previously characterized EE driver); and (3) 44 drivers containing enhancers we identified as originating within 10kb of the genes for the midgut-secreted peptides Allatostatin A, Allatostatin C, Bursicon, CCHamide-1, Diuretic hormone 31, Insulin-like peptide 3,

Myoinhibiting peptide precursor, Slit, and Tachykinin (Veenstra et al. 2008; Veenstra 2009; Nässel and Winther 2010; Veenstra and Ida 2014; Guo et al. 2019; Hung et al. 2020; Zhou et al. 2020). A total of 41 AD drivers and 47 DBD drivers were screened using the corresponding R57F07.A driver and a UAS-*Stinger* reporter. While most of the drivers induced UAS-*Stinger* expression in fewer EE cells than the R57F07.A driver pair, we identified a single AD driver that induced expression in a particularly high number of EEs. We present our characterization of this unique driver below.

Characterization of a novel enteroendocrine cell driver pair

The driver of interest identified by our screen uses the R20C06 enhancer fragment to direct *p65AD* expression. To evaluate the utility of R20C06 for detection of EEs, we examined UAS-*Stinger* expression in detail when R20C06-*p65AD* was combined with R20C06-GAL4DBD. We observed expression directed by this driver pair in substantially more EEs than induced by the previously characterized R57F07.A-*p65AD* and -GAL4DBD driver pair (Ariyapala et al. 2020) and the expression was nearly exclusive to EEs based on anti-Pros antibody staining (Figs. 1 and 2). In intestinal regions R1 and R2, no expression driven by the R20C06 driver pair was observed in other cell types, and R3, R4, and R5 showed non-EE expression in only 2%, 7%, and 2% of *Stinger*-positive cells, respectively. (These *Stinger*-positive, Pros-negative cells have small nuclei, which suggests they are a subset of progenitor cells.) R57F07.A split-GAL4 drivers together drove no expression in non-EE cells in R2, R3, and R4, and drove expression in non-EEs in 1% of *Stinger*-positive cells in R1 and 24% in R5, with many of the R5 *Stinger*-positive, Pros-negative cells having large nuclei (likely ECs). This indicates that both driver pairs conferred quite low levels of UAS-*Stinger* expression in non-EEs, while the R20C06 pair drove expression in a greater proportion of EEs (approximately 45% more on average). Although some GAL4 drivers with equivalent or superior EE detection capabilities have been identified, such as P{*GawB*}*pros*^{V1} (Scopelliti et al. 2014) and TI{2A-GAL4}CG32547^{2A-GAL4} (Guo et al. 2019), this is the most comprehensive detection of EE cells reported to date using any split-GAL4 driver pair.

We examined R20C06-*p65AD* in our screen because, curiously, Ariyapala et al. (2020) saw that it drove a distinctly different EE expression pattern than R20C06-GAL4DBD, even though these 2 transgenes share an enhancer fragment. They reported no intestinal UAS reporter expression in undissected adults when R20C06-*p65AD* was combined with the intestine-specific CG10116-GAL4DBD driver, even though R20C06-GAL4DBD drove clear UAS reporter expression when combined with CG10116-*p65AD*. This unusual difference prompted us to look closely at dissected intestines from flies with R20C06-*p65AD* combined with CG10116-GAL4DBD. While we saw a small number of cells in R1a adjacent to the proventriculus expressing UAS-*Stinger* (Supplementary Fig. 2), it is not surprising that expression in so few cells was missed in the previous high-throughput primary screen, which relied on detecting intestinal fluorescence in undissected adults. This pattern is unexpectedly limited, given how extensively these drivers are known to be expressed in EEs from other experiments. It suggests that the expression of one or both drivers is inhibited in this particular genotype, but we have not investigated it further since R20C06-*p65AD* expression appeared otherwise straightforward in the experiments described below. Ariyapala et al. (2020) had also shown that the combination of R20C06-GAL4DBD and R57F07.A-*p65AD* directed UAS reporter expression in EEs but had observed fewer EE cells with expression

than we saw with R20C06-*p65AD* and R57F07.A-GAL4DBD, particularly in the center of R4. Taken together, these observations show why the R20C06 drivers were not identified as especially promising EE drivers in the previous study.

To further confirm the EE specificity of the R20C06-*p65AD* and R20C06-GAL4DBD drivers, we combined them with the cell-type specific drivers used in Ariyapala et al. (2020) for progenitor cells, ECs, and EBs (Fig. 3). The results were consistent with our expectation that these driver pairs would not direct expression in non-EE midgut cells aside from a single exception; namely, that R20C06-GAL4DBD drove occasional UAS-*Stinger* expression in large nuclei (likely ECs) when combined with the reference EC-*p65AD* driver. This expression was observed primarily in R1, but it was also seen sporadically in other regions (Fig. 3g). Ariyapala et al. (2020) saw UAS reporter expression in cells with large nuclei (likely ECs) when several split-GAL4 drivers were combined with the reference R57F07.A drivers, including when the R57F07.A-*p65AD* and -GAL4DBD reference drivers were combined (also visible in Fig. 1a), so it was not surprising to see similar expression when R20C06-GAL4DBD was combined with EC-*p65AD*. Nevertheless, no other driver showed EC-like expression with the R20C06 drivers (described below), indicating that expression of the R20C06 drivers was more specific to EEs than expression of the R57F07.A drivers.

We also saw R20C06-*p65AD* and R20C06-GAL4DBD drivers directing EE expression when combined with the EC reference drivers. In these combinations, we saw UAS-*Stinger* expressed in populations of small cells in R3, particularly near the boundaries with R2 and R4 (Fig. 3c inset and g right inset). We confirmed that these cells were EEs based on anti-Pros antibody staining (Supplementary Fig. 3). Ariyapala et al. (2020) saw a similar pattern of expression in EEs in R3 with 25 driver combinations involving the EC reference drivers. Examples of these include EC-*p65AD* combined with R21H01-GAL4DBD or R46F04-GAL4DBD, as well as EC-GAL4DBD combined with VT021418-*p65AD*. These results highlight a minor weakness with the EC reference drivers but are consistent with nearly exclusive EE expression of the R20C06 drivers.

In addition to the R20C06 drivers directing UAS-*Stinger* expression in typical EE cells, we saw that R20C06-*p65AD* drove UAS reporter expression in EEs at the anterior and posterior boundaries of R3 in combination with the *Progenitor*-GAL4DBD reference driver (Fig. 3b inset). Hung et al. (2020) showed that cells in these locations constitute a unique subpopulation of EEs expressing both neuropeptide hormones and genes usually restricted to progenitor cells (but, notably, not *Delta*, the gene most closely associated with progenitor cell identity). Fig. 4, a–c show that all cells identified by these drivers were labeled by both a marker for EE cells, anti-Pros antibody (Shiga et al. 1996; Micchelli and Perrimon 2006), and markers for progenitor cells, anti-HRP antibody (O'Brien et al. 2011; Miller et al. 2020) and a GFP reporter for the *escargot* gene called TI{*sfGFP*}*esg*^{K1} (Micchelli and Perrimon 2006).

In contrast, R20C06-GAL4DBD combined with *Progenitor*-*p65AD* did not direct expression of UAS-*Stinger* in this special EE subpopulation (Fig. 3f inset), a difference that likely reflects the fact that the enhancer fragment in *Progenitor*-GAL4DBD (VT024642) is different than that in *Progenitor*-*p65AD* (VT004241). We similarly saw no UAS-*Stinger* expression in these cells when R57F07.A-GAL4DBD was combined with *Progenitor*-*p65AD*, even though we saw expression when R57F07.A-*p65AD* was combined with *Progenitor*-GAL4DBD that was very similar to the expression we saw when we combined R20C06-*p65AD* with *Progenitor*-GAL4DBD (Fig. 4, d and e). Ariyapala et al. (2020) reported another driver (R10F08-*p65AD*) that

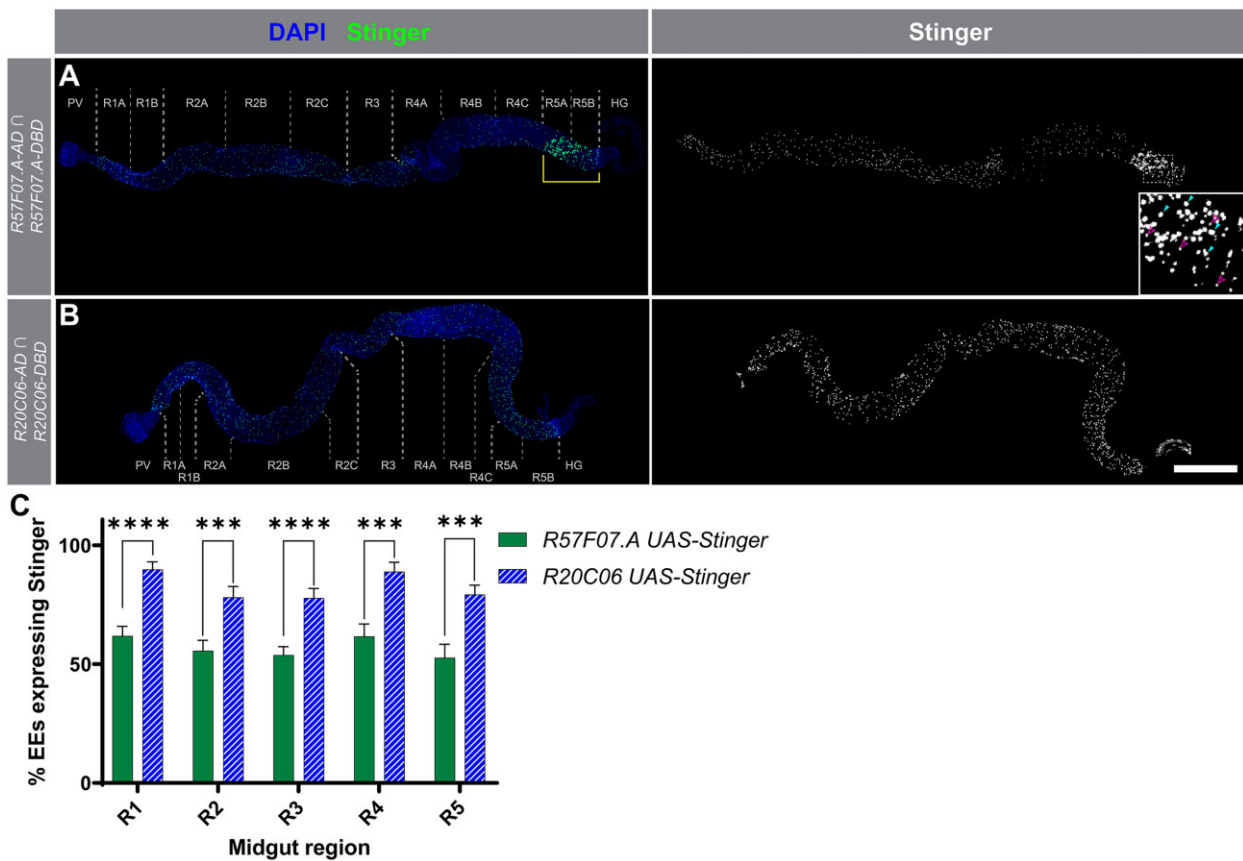


Fig. 1. R20C06 split-GAL4 drivers directed expression in more EEs than R57F07.A split-GAL4 drivers. a, b) These micrographs show UAS-Stinger expression (right column; superimposed on DAPI nuclear counterstaining in the left column) driven by the R57F07.A or R20C06 split-GAL4 driver pairs. Regional boundaries used in expression pattern analysis throughout the study are indicated. Scale bar 500 μ m. a) R57F07.A drivers directed expression throughout the gut but drove expression in only ~60% of EEs. They also drove unexpected expression in large nuclei (likely ECs) in R5 (indicated by bracket). The inset shows an enlargement of the indicated portion of R5, with examples of large nuclei highlighted by filled arrowheads and small nuclei highlighted by open arrowheads. b) R20C06 drivers directed expression evenly throughout all gut regions and did not drive expression in large nuclei. c) This graph summarizes the percentage of EEs detected by each driver pair and illustrates that, although R20C06 drivers did not direct expression in all EEs, they directed expression in a significantly larger percentage of EEs than the R57F07.A drivers in each midgut region. *** $P < 0.001$, **** $P < 0.0001$.

detected this EE subpopulation in combination with the *Progenitor-GAL4DBD* driver as well. All together, these results suggest that the *Progenitor-GAL4DBD* reference driver is a useful tool for marking this subpopulation.

Reporter effects on expression patterns

The EE characterization and screening data reported by Ariyapala et al. (2020) were collected using *PBac{UAS-DSCP-6XEGFP}* reporters combined with R57F07.A drivers. The extremely bright fluorescence of these UAS-6xGFP reporters, arising from 20 copies of UAS and 6 copies of the GFP coding sequence, was appropriate for that screen but was not necessary for the current study. Instead, we used the UAS-Stinger reporters because they are clear and easy to detect without the need for antibody staining yet are not so bright that it is difficult to distinguish individual cells. To evaluate whether these different reporters provided consistent results when combined with the EE reference driver pairs, we examined EE fluorescence when the R57F07.A and R20C06 driver pairs were combined with the UAS-6xGFP and UAS-Stinger reporters. When both driver pairs were characterized, we saw similar numbers of fluorescent EE cells with UAS-Stinger and UAS-6xGFP in all midgut regions, but with slightly more fluorescent cells observed with UAS-Stinger (Fig. 5). This marginal difference between UAS-Stinger and UAS-6xGFP expression reached

statistical significance only in R2, R3, and R4 when driven by the R20C06 drivers (Fig. 5b). These results suggest that UAS-Stinger reports slightly more comprehensive expression patterns than UAS-6xGFP with EE reference drivers.

Furthermore, as described in the previous section, the use of UAS-Stinger allowed us to identify an expression pattern resulting from a combination of R57F07.A and *Progenitor-GAL4DBD* drivers that had been undetectable using UAS-6xGFP. Additional study is necessary to determine the cause of this difference, but it is consistent with previous studies showing that both high levels of p65AD and reporter protein expression from 10 or more UAS sites can be toxic to cells (Pfeiffer et al. 2010). Taken together, these similarities and differences between UAS-Stinger and UAS-6xGFP underscore the importance of careful reporter selection and characterization.

Characterization of the R20C06 enhancer fragment

In an attempt to identify additional tools useful for the study of EEs, we examined other drivers and cell markers related to the R20C06 enhancer fragment. We compared the midgut expression pattern of the split-GAL4 R20C06 driver pair to that of the GAL4 driver containing the same enhancer fragment using a UAS-Stinger reporter (Fig. 6, a and b). The GAL4 driver showed a

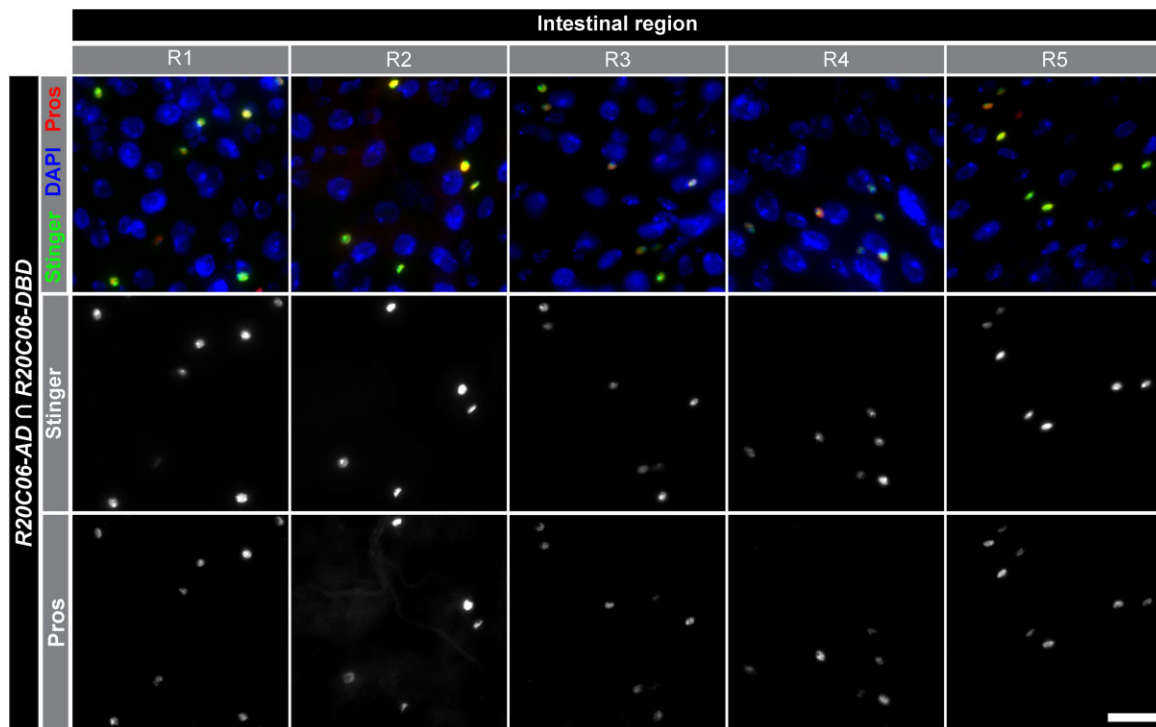


Fig. 2. R20C06 drivers predominantly labeled EE cells. UAS-Stinger expression in intestinal regions R1–5 directed by R20C06 drivers (center row) occurs largely in EEs, which are identified by anti-Pros staining (bottom row). Stinger expression and anti-Prospero staining are shown superimposed on DAPI nuclear counterstaining in the top row. Scale bar 20 μ m.

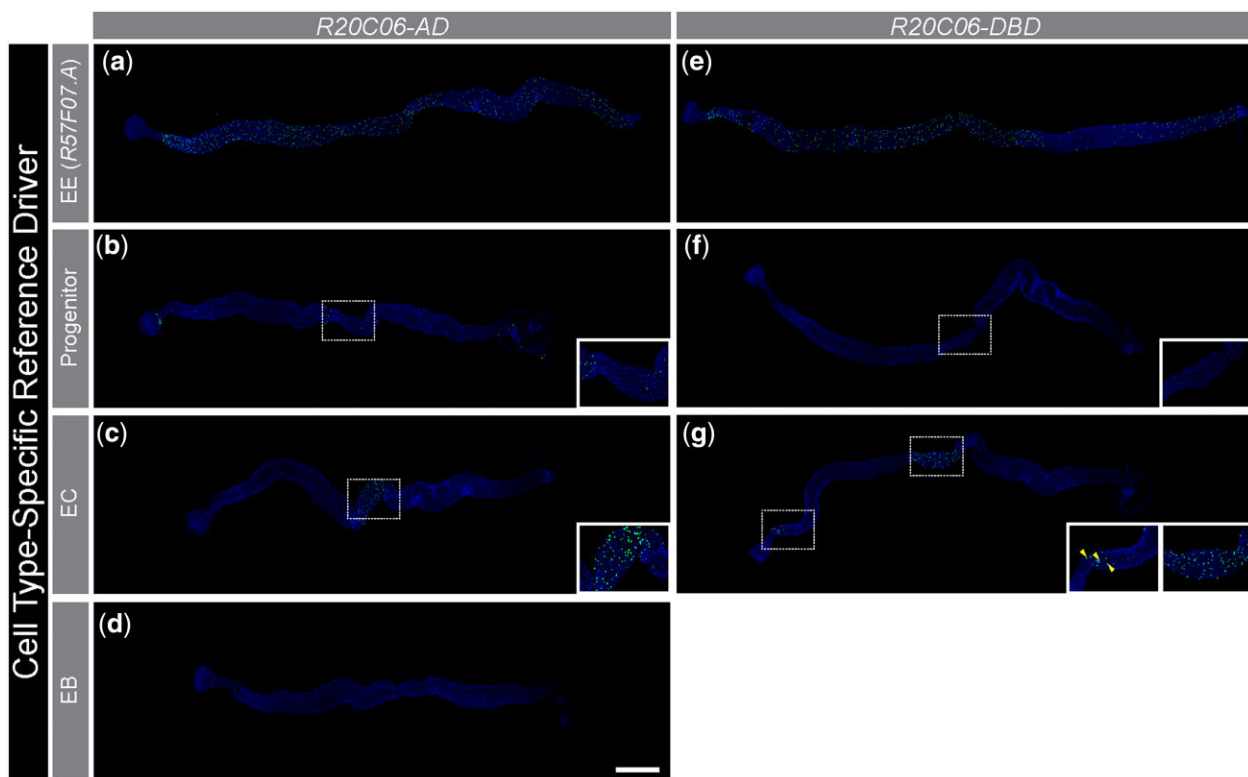


Fig. 3. R20C06 drivers labeled only a few non-EE cells. R20C06-p65AD and R20C06-GAL4DBD drove intestinal EE expression of UAS-Stinger in combination with the R57F07.A EE reference drivers (a, e) and drove little to no reporter expression in non-EE cells when combined with progenitor cell (b, f), EC (c, g), or EB (d) reference drivers. Unexpected reporter expression in EEs was seen, primarily in the central midgut, when the R20C06-p65AD driver was combined with the Progenitor-GAL4DBD driver (b; see Fig. 4 for details), and when either of the R20C06 drivers was combined with an EC reference driver (c, g right inset; Supplementary Fig. 2). The only instance of unexpected reporter expression involving non-EE cells was observed in large nuclei (likely ECs) when R20C06-GAL4DBD was combined with EC-p65AD (g left inset, example of large nuclei highlighted by arrowheads). Insets show enlargements of the indicated regions. All intestines are shown with DAPI nuclear counterstaining. Scale bar 500 μ m.

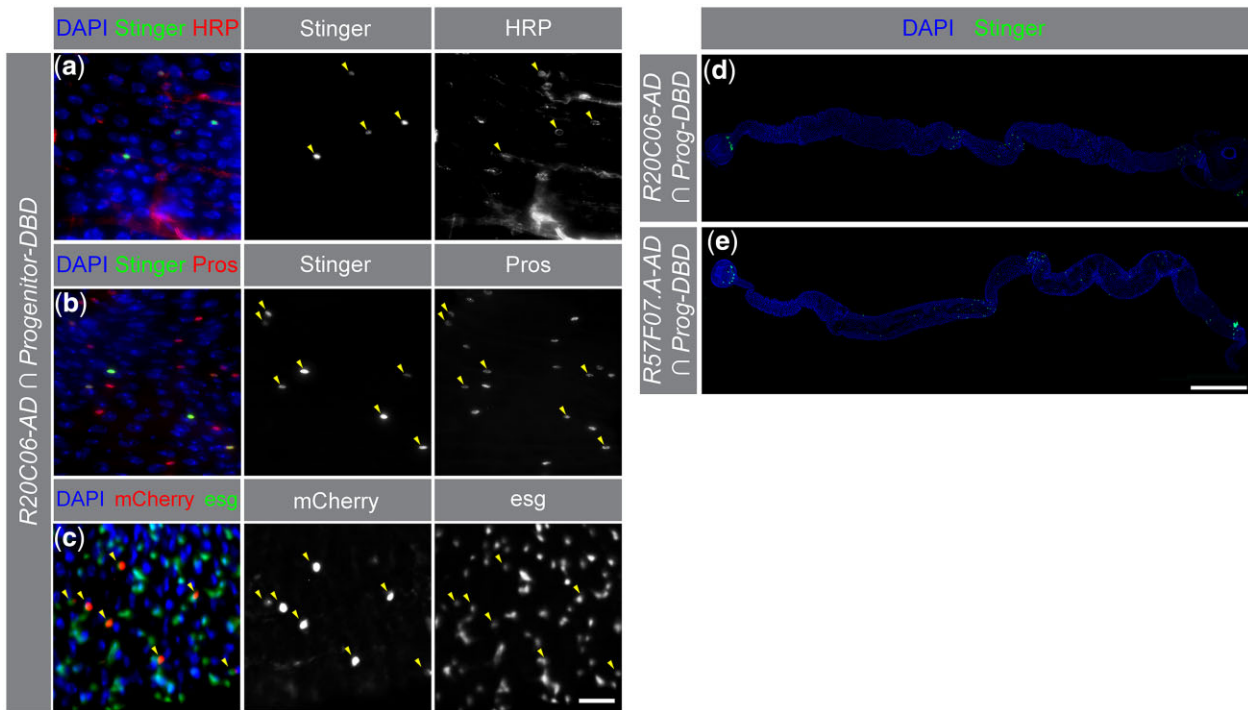


Fig. 4. R20C06-p65AD drove reporter expression in a unique group of EEs. a–c) When R20C06-p65AD was combined with the *Progenitor-GAL4DBD* reference driver and a UAS reporter (UAS-*Stinger* or UAS-*mCherry*, center column), the subset of cells that displayed UAS reporter expression also showed staining for both (a) the progenitor cell marker anti-HRP and (b) the EE cell marker anti-Pros (right column), indicating that these cells are part of a unique EE subpopulation identified by Hung et al. (2020). These cells also express the progenitor cell marker $Tl\{sfGFP\}esg^{KI}$, which places GFP expression under the control of *escargot* (*esg*) regulatory sequences (c, right column). The left column shows the patterns in the center and right columns superimposed on DAPI nuclear counterstaining. Scale bar 20 μm . (d, e) R20C06-p65AD and R57F07.A-p65AD drove similar patterns of UAS-*Stinger* expression (superimposed on DAPI nuclear counterstaining) when combined with *Progenitor-GAL4DBD*. R57F07.A-p65AD drove additional expression in the proventriculus and the hindgut (e). Scale bar 500 μm .

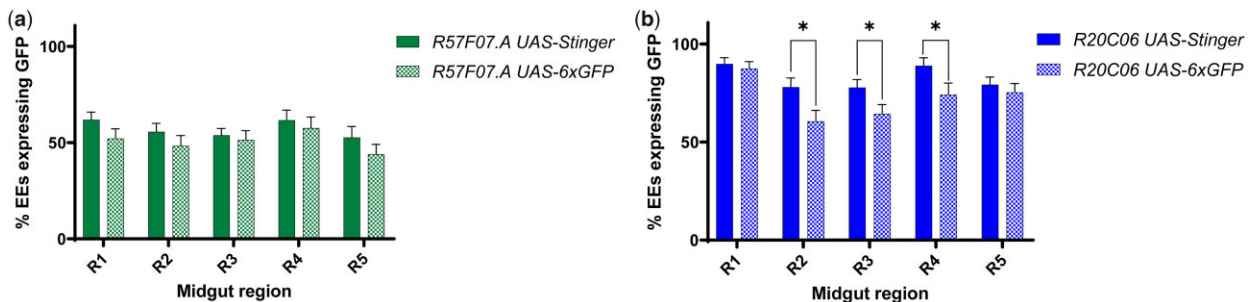


Fig. 5. UAS-*Stinger* was a slightly more effective reporter than UAS-6xGFP in combination with EE reference drivers. a) When the R57F07.A drivers were characterized, there was a slight tendency toward more cells with fluorescence in all midgut regions with a UAS-*Stinger* reporter than a UAS-6xGFP reporter. b) This pattern was also observed when characterizing the R20C06 drivers, with UAS-*Stinger* expressed in significantly more cells than UAS-6xGFP in R2, R3, and R4. * $P < 0.05$.

notably more restricted expression pattern than the split-GAL4 pair: the GAL4 driver displayed very little expression in R2 and R4 while the split-GAL4 pair showed evenly distributed expression through all 5 of the major midgut regions. This is not entirely surprising, as idiosyncratic differences between GAL4 and split-GAL4 drivers have been observed in other instances as well (Luan et al. 2006; Pfeiffer et al. 2010; Ariyapala et al. 2020). Pfeiffer et al. (2010) suggested that split-GAL4 drivers may direct more widespread expression than their cognate GAL4 drivers due to the use of the stronger p65 activation domain. Regardless, these results indicate that R20C06-GAL4 is not as well suited for use as a pan-EE driver as the corresponding split-GAL4 drivers.

The R20C06 enhancer fragment lies within the nicotinic Acetylcholine Receptor $\alpha 5$ (*nAChR $\alpha 5$*) gene and there are no other genes within 16 kb of this fragment (Larkin et al. 2021). To investigate possible relationships between the midgut expression patterns of the R20C06 drivers and *nAChR $\alpha 5$* , we compared driver expression to relevant intestinal RNAseq data (Guo et al. 2019; Hung et al. 2020) and to the expression of protein-trap and gene-trap insertions associated with *nAChR $\alpha 5$* . RNAseq data shows that *nAChR $\alpha 5$* is expressed in a variety of EE types throughout the gut (Guo et al. 2019) and that the gene is expressed in the largest number of cells in R4 and R5 (Dutta et al. 2013). When we examined the expression pattern of $Mi\{Trojan-GAL4.2\}nAChR\alpha 5^{MI13859-TG4.2}$, a gene trap for *nAChR $\alpha 5$* ,

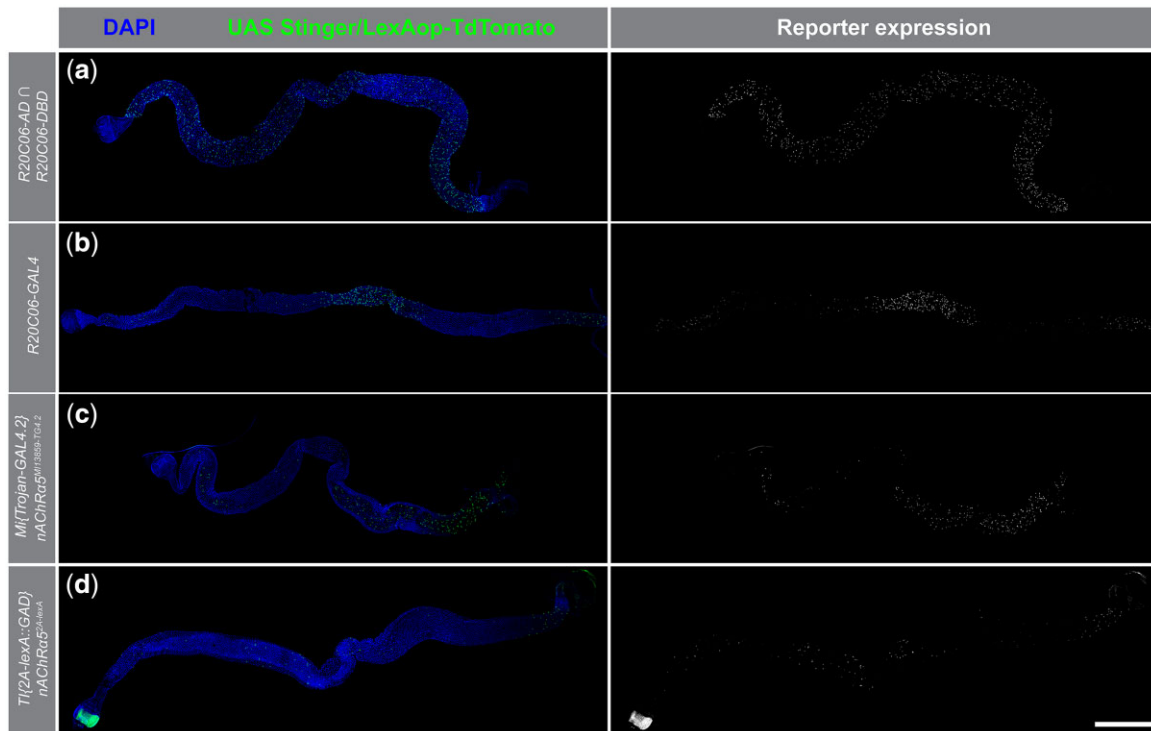


Fig. 6. R20C06 split-GAL4 drivers conferred different expression patterns than the R20C06-GAL4 driver or *nAChR α 5*-associated gene-trap drivers. Split-GAL4 drivers with the R20C06 enhancer fragment showed expression throughout the entire midgut (a), while the GAL4 driver using the same enhancer fragment showed expression primarily R1, R3, and R5 (b). The *Mi{Trojan-GAL4.2}*nAChR α 5*^{MI13859-TG4.2}* GAL4 gene-trap driver showed expression primarily in the posterior midgut (R4 and R5) with additional expression in scattered cells in the anterior and middle midgut (c). The *Tl{2A-lexA::GAD}*nAChR α 5*^{2A-lexA}* *lexA* gene-trap driver (d) directed expression similar to that of the R20C06-GAL4 driver (c), but drove expression in fewer cells. Proventricular expression of *PBac{13XLexAop2-IVS-tdTomato.nls}VK00022* occurs even in the absence of a *lexA* driver (data not shown). *UAS-Stinger* (a–c) and *lexAop-tdTomato.nls* (d) expression are shown in the right column, and superimposed on nuclear DAPI staining in the left column. Scale bar 500 μ m.

with a *UAS-Stinger* reporter, we saw expression that corresponded to the RNAseq data: expression in the greatest number of cells in the posterior midgut with additional expression in fewer cells in the anterior midgut (Fig. 6c). When we examined *lexAop-tdTomato.nls* expression driven by *Tl{2A-lexA::GAD}*nAChR α 5*^{2A-lexA}*, a gene-trap insertion expressing *lexA* (Fig. 6d), we observed a similar pattern to that of R20C06-GAL4, but with expression in fewer cells. In addition, we analyzed the *nAChR α 5* protein-trap insertion *Mi{PT-GFSTF.0}*nAChR α 5*^{MI05549-GFSTF.0}*, but we were not able to detect any expression in the midgut epithelium using immunostaining against GFP (data not shown). Based on these observations, the R20C06 split-GAL4 drivers behave differently than GAL4 drivers containing the same enhancer fragment and the protein and gene traps for the nearby *nAChR α 5* gene. Therefore, these other genetic elements do not present promising avenues for future pan-EE tool development. More broadly speaking, these results reemphasize that isolated enhancers or enhancer fragments are often not sufficient to recapitulate the native expression of genes and that the expression patterns driven by enhancers also depend on adjacent sequences and genomic contexts.

Other split-GAL4 drivers that detect enteroendocrine cells in the *Drosophila* midgut

During the screen that identified the R20C06 split-GAL4 driver pair, we collected expression pattern data for all the split-GAL4 drivers screened with R57F07.A. We later combined all drivers from that initial screen with the R20C06 drivers so that we could evaluate differences and similarities in expression patterns and explore the utility of the R20C06 driver pair for EE detection in the split-GAL4 system. Overall, 88 split-GAL4 drivers were tested.

There were 42 drivers (48%) positive for adult midgut expression when crossed to the R57F07.A drivers and 39 drivers (44%) positive when crossed to the R20C06 drivers (Supplementary Table 3). All expression pattern data from these screens are available at https://bdsc.indiana.edu/stocks/gal4/midgut_EEs.html.

There were 3 drivers (R75B09-GAL4DBD, R47G08-GAL4DBD, R27B07-GAL4DBD) which activated *UAS-Stinger* expression when crossed to an R57F07.A driver but not when crossed to a R20C06 driver, while only one driver (R65D06-GAL4DBD) activated *UAS-Stinger* expression when crossed to a R20C06 driver but not when crossed to a R57F07.A driver. Drivers expressing with both R57F07.A and R20C06 fell into 3 classes: (1) 64 drivers showed similar patterns when crossed to either reference driver (Fig. 7a); (2) 12 drivers gave expression in more cells with the R20C06 than the R57F07.A reference driver (Fig. 7b); and (3) 7 drivers gave expression in more cells with the R57F07.A than the R20C06 reference driver (Fig. 7c). It is important to note that even if a driver is in category 1, more research is necessary to verify that identical cell populations are being identified by both drivers. In addition, crosses with R20C06 did not show any expression in big nuclei (likely ECs), while this was somewhat common in crosses with R57F07.A (e.g. R5 in Fig. 7d). These results indicated that, overall, both R57F07.A and R20C06 drivers detected many EEs in the adult midgut. The R57F07.A drivers directed expression in a few situations that R20C06 drivers did not, but the R20C06 drivers conferred other advantages, such as less non-EE expression and more combinations expressing in a greater number of EEs.

We also examined adult brains from split-GAL4 combinations that drove expression in EEs. Because brains were dissected only in cases where midgut *UAS-Stinger* expression was present, the

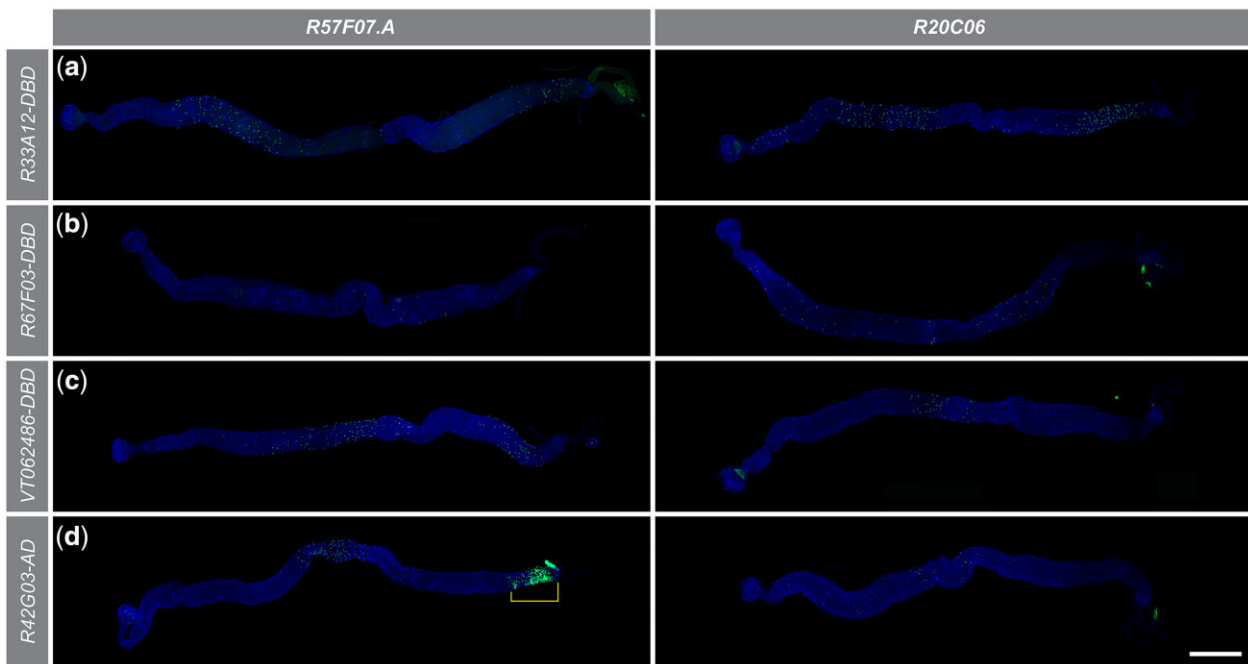


Fig. 7. R57F07.A and R20C06 reference drivers directed different expression patterns when combined with the same experimental split-GAL4 driver. These micrographs show representative examples of UAS-Stinger expression (green) when split-GAL4 drivers were combined with the corresponding R57F07.A (left) or R20C06 (right) split-GAL4 driver. a) R33A12-GAL4DBD drove similar patterns when combined with both reference drivers. b) R67F03-GAL4DBD drove more expression when combined with R20C06-p65AD than with R57F07.A-p65AD. c) VT062486-GAL4DBD drove more expression when combined with R57F07.A-p65AD than with R20C06-p65AD. d) R42G03-p65AD drove similar expression patterns when combined with both reference drivers, but also drove expression in large nuclei (likely ECs) with R57F07.A-GAL4DBD as indicated by bracket. Scale bar 500 μ m.

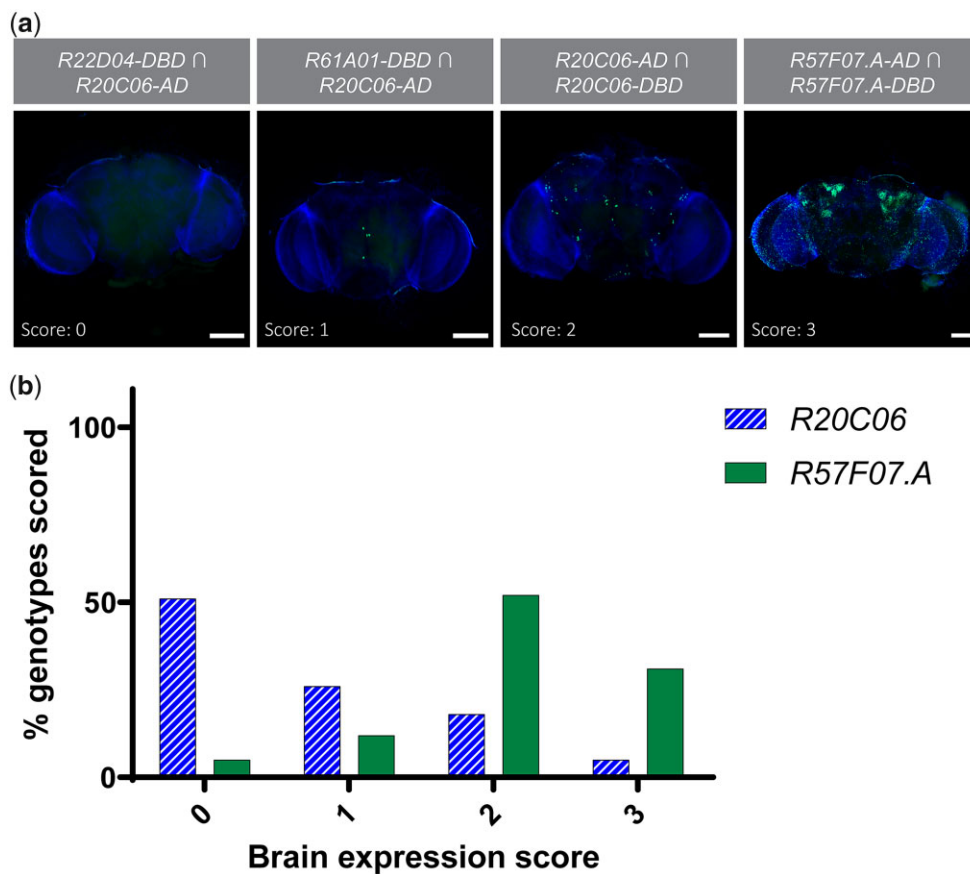


Fig. 8. R20C06 drivers direct less expression in the brain than R57F07.A drivers. a) Representative examples of each score are shown, with UAS-Stinger expression shown superimposed on nuclear DAPI counterstaining. Brains were scored on a scale of 0 to 3, where 0 indicated no clear reporter expression, 1 indicated a few (≤ 9) cells with expression, 2 indicated a moderate number of cells (10–60) with expression, and 3 indicated many cells (> 60) with expression. Scale bars 100 μ m. b) The 36 split-GAL4 combinations involving R20C06 drivers showed a significantly stronger propensity toward lower scores than the 42 combinations involving R57F07.A drivers ($P < 0.001$).

total number of genotypes with brains scored varied slightly between R20C06 and R57F07.A drivers. We scored brains from 39 driver pairs using R20C06 and 42 driver pairs using R57F07.A on a semiquantitative scale from 0–3, with 0 indicating no expression and 3 indicating a large number of cells with expression (Fig. 8a). When we analyzed brains from progeny of R57F07.A crosses, 17% of genotypes examined had a score of 1 or 0 (little to no expression), while 77% of genotypes from crosses involving R20C06 drivers had a score of 1 or 0. Conversely, only 5% of genotypes with R20C06 drivers received a score of 3 (large number of cells with expression) whereas 31% genotypes with R57F07.A drivers had a score of 3 (Fig. 8b, Supplementary Table 3). These results demonstrated that R20C06 drivers directed significantly less reporter expression in the brain, which suggests that these drivers are more useful tools than R57F07.A drivers for disentangling the physiological roles of hormone-secreting cells in the gut from those secreting the same peptides in the brain.

In summary, combinations of experimental drivers and the 2 corresponding reference drivers can, in some cases, drive distinctly different EE expression patterns. The differences between the R20C06 and R57F07.A drivers expand available options and allow researchers to select the reference drivers more suitable to a given EE population of interest. Further research is necessary to characterize these EE-specific reference drivers more deeply, understand their similarities and differences in greater detail, and elaborate on the advantages unique to each driver pair.

Data availability

The accompanying tables contain complete characterization data. Supplementary Table 1 contains antibody details and genotypes for each strain used. Supplementary Table 2 provides the rationale for inclusion of drivers in the screen. Supplementary Table 3 contains characterization data collected in the screen. Supplementary Table 4 lists the genotypes of all strains shown in figures. Intestine images and screen data are available at https://bdsc.indiana.edu/stocks/gal4/midgut_EEs.html. Extant stocks are available from the Bloomington Drosophila Stock Center (<https://bdsc.indiana.edu>) or upon request.

Supplemental material is available at G3 online.

Acknowledgments

The authors thank Annette Parks and Jim Smotherman for help constructing the associated webpages; Ishara Ariyapala, Thom Kaufman, Nicholas Sokol, and Cale Whitworth for helpful discussion; and FlyBase for genetic and genomic information provided under National Institutes of Health grant U41 HG000739 and funding from the British Medical Research Council.

Funding

This work was supported by National Institutes of Health grants P40 OD018537 and R21 OD026525.

Conflicts of interest

None declared.

Literature cited

- Ariyapala IS, Holsopple JM, Popodi EM, Hartwick DG, Kahsai L, Cook KR, Sokol NS. Identification of split-GAL4 drivers and enhancers that allow regional cell type manipulations of the *Drosophila melanogaster* intestine. *Genetics*. 2020;216(4):891–903.
- Beehler-Evans R, Micchelli CA. Generation of enteroendocrine cell diversity in midgut stem cell lineages. *Development*. 2015;142(4):654–664.
- Buchon N, Osman D, David FPA, Fang HY, Boquete J-P, Deplancke B, Lemaître B. Morphological and molecular characterization of adult midgut compartmentalization in *Drosophila*. *Cell Rep*. 2013;3(5):1725–1738.
- Dionne H, Hibbard KL, Cavallaro A, Kao JC, Rubin GM. Genetic reagents for making split-GAL4 lines in *Drosophila*. *Genetics*. 2018;209(1):31–35.
- Dutta D, Xiang J, Edgar BA. RNA expression profiling from UNIT 2F.2 FACS-isolated cells of the *Drosophila* intestine. *Curr Protoc Stem Cell Biol*. 2013;1:2F.2.1–2F.2.12.
- Guo X, Yin C, Yang F, Zhang Y, Huang H, Wang J, Deng B, Cai T, Rao Y, Xi R, et al. The cellular diversity and transcription factor code of *Drosophila* enteroendocrine cells. *Cell Rep*. 2019;29(12):4172–4185.
- Hung R-J, Hu Y, Kirchner R, Liu Y, Xu C, Comjean A, Tattikota SG, Li F, Song W, Ho Sui S, et al. A cell atlas of the adult *Drosophila* midgut. *Proc Natl Acad Sci USA*. 2020;117(3):1514–1523.
- Larkin A, Marygold SJ, Antonazzo G, Attrill H, Dos Santos G, Garapati PV, Goodman JL, Gramates LS, Millburn G, Strelets VB, et al.; FlyBase Consortium. FlyBase: updates to the *Drosophila melanogaster* knowledge base. *Nucleic Acids Res*. 2021;49(D1):D899–D907.
- Lim SY, You H, Lee J, Lee Y, Lee K-A, Kim B, Lee J-H, Jeong J, Jang S, et al. Identification and characterization of GAL4 drivers that mark distinct cell types and regions in the *Drosophila* adult gut. *J Neurogenet*. 2021;35(1):33–44.
- Luan H, Peabody NC, Vinson CRR, White BH. Refined spatial manipulation of neuronal function by combinatorial restriction of transgene expression. *Neuron*. 2006;52(3):425–436.
- Marianes A, Spradling AC. Physiological and stem cell compartmentalization within the *Drosophila* midgut. *Elife*. 2013;2013:1–19.
- Micchelli CA, Perrimon N. Evidence that stem cells reside in the adult *Drosophila* midgut epithelium. *Nature*. 2006;439(7075):475–479.
- Miguel-Aliaga I, Jasper H, Lemaître B. Anatomy and physiology of the digestive tract of *Drosophila melanogaster*. *Genetics*. 2018;210(2):357–396.
- Miller DE, Kahsai L, Buddika K, Dixon MJ, Kim BY, Calvi BR, Sokol NS, Hawley RS, Cook KR. Identification and characterization of breakpoints and mutations on *Drosophila melanogaster* balancer chromosomes. *G3 (Bethesda)*. 2020;10(11):4271–4285.
- Nässel DR, Winther ÅME. *Drosophila* neuropeptides in regulation of physiology and behavior. *Prog Neurobiol*. 2010;92(1):42–104.
- O'Brien LE, Soliman SS, Li X, Bilder D. Altered modes of stem cell division drive adaptive intestinal growth. *Cell*. 2011;147(3):603–614.
- Ohlstein B, Spradling A. The adult *Drosophila* posterior midgut is maintained by pluripotent stem cells. *Nature*. 2006;439(7075):470–474.
- Pfeiffer BD, Ngo T-TB, Hibbard KL, Murphy C, Jenett A, Truman JW, Rubin GM. Refinement of tools for targeted gene expression in *Drosophila*. *Genetics*. 2010;186(2):735–755.
- Scopelliti A, Cordero JB, Diao F, Strathdee K, White BH, Sansom OJ, Vidal M. Article local control of intestinal stem cell homeostasis

- by enteroendocrine cells in the adult *Drosophila* midgut. *Curr Biol*. 2014;24(11):1199–1211.
- Shiga Y, Tanaka-Matakatsu M, Hayashi S. A nuclear GFP/beta-galactosidase fusion protein as a marker for morphogenesis in living *Drosophila*. *Dev Growth Differ*. 1996;38(1):99–106.
- Veenstra JA. Peptidergic paracrine and endocrine cells in the midgut of the fruit fly maggot. *Cell Tissue Res*. 2009;336(2):309–323.
- Veenstra JA, Agricola HJ, Sellami A. Regulatory peptides in fruit fly midgut. *Cell Tissue Res*. 2008;334(3):499–516.
- Veenstra JA, Ida T. More *Drosophila* enteroendocrine peptides: orckinin B and the CCHamides 1 and 2. *Cell Tissue Res*. 2014;357(3):607–621.
- Zhou X, Ding G, Li J, Xiang X, Rushworth E, Song W. Physiological and pathological regulation of peripheral metabolism by gut-peptide hormones in *Drosophila*. *Front Physiol*. 2020;11:577717.
- Zwick RK, Ohlstein B, Klein OD. Intestinal renewal across the animal kingdom: comparing stem cell activity in mouse and *Drosophila*. *Am J Physiol Gastrointest Liver Physiol*. 2019;316(3):G313–G322.

Communicating editor: A. Bashirullah